# Precise Radial Velocity Estimation for Inverse Synthetic Aperture Radar

**Jianzhi Lin\*, Yue Zhang, Weixing Li, and Zengping Chen**

**Abstract**—This paper describes a convenient technique of precise radial velocity estimation for inverse synthetic aperture radar (ISAR). In order to keep both the range profile and phase history of the echoes coherent, direct sampling with high sampling rate using high performance analog-to-digital converter and matched-filter correlation processing in pulse compression are used for the ISAR system. Due to the coherence property of the echoes, the translational motion compensation parameters for ISAR imaging are just the radial motion parameters of the target. Thus, the coarse velocity estimation is obtained by range alignment and fine velocity estimation is achieved by phase adjustment. The fine velocity estimation is ambiguous and the coarse velocity estimation is used for ambiguity resolution. The advantage of this technique is the high precision with range error values at sub wavelength levels, and it achieves velocity information and translational motion compensation at the same time. Both simulated and experimental validations are presented to verify the effectiveness of the proposed method.

## 1. INTRODUCTION

Inverse synthetic aperture radar (ISAR) has rapid development all over the world, owing to its ability to provide two-dimensional high-resolution images of moving targets in all-weather, and night and day circumstances.

In radar, it is always crucial to estimate the radial range or velocity between the radar and a target. This can be a precursor to more detailed signal processing whose end product might be a radar image of the object, or a Doppler spectrum extraction of the target [1]. Thus the ISAR system is usually accompanied by a narrowband mode or narrowband radar, which conducts the functions of searching and tracking the target but rarely provides precision high enough for the target velocity while inducing implementation difficulties in the radar system. An alternative solution is to estimate velocity directly from the wideband echo by signal processing, which has the advantage of decreasing the burden of the radar system, and this work has attracted much attention in the radar community [2–21].

A highly precise measurement of range or velocity based on radar phase named Phase-Derived Range was applied to missile defense systems, which had proven the capability of estimating precession parameters [3–6]. However, the details of the technique have not been published. Accurate velocity estimation methods for wideband radar based on keystone transform were proposed [7–9]. But they were only suitable for targets with uniform motion. Some researches focused on motion compensation for high resolution range profile (HRRP) but the estimated velocity was low precision [2, 10, 11]. A novel method of precise radial range measurement based on dechirped echoes was presented in [12]. However, it was difficult in phase extraction and ambiguity resolution. Moreover, it needed high precise velocity as a precursor. Recently, the work has been extended to direct sampling radar [13], but the disadvantage still exits. Some investigations were relied on signal waveforms [14–16] or system structures [17, 18]. A

method not based on range profile was presented in [19], but it suffered from heavy computation load. An efficient algorithm for maximum likelihood estimation of translational motion was described in [20]; however, it assumed that the maximum relative translational motion from pulse to pulse was less than one wavelength. A basic, simple and reliable approach for estimation and compensation of the target relative translational motion was proposed in [21], but the correct behaviour of the algorithm depended on its correct initialisation.

With the development of analog-to-digital converter, direct sampling with high sampling rate and matched-filter correlation processing in pulse compression for ISAR become realistic [22]. Compared to dechirping (or stretch) processing, matched-filter correlation processing can keep both the HRRP and phase history of the echoes coherent [23]. Thus the translational motion compensation parameters for ISAR imaging are just the radial motion parameters of the target. Hence, the velocity information can be obtained while the translational motion is compensated.

In this paper, a convenient method of precise radial velocity estimation is proposed. The method is based on the coherent property of the echoes. In the first step, range alignment is applied to get the range shift, which is proportional to the coarse velocity. In the second step, phase adjustment is taken to obtain the ambiguous range shift, which is proportional to the fine but ambiguous velocity. In the third step, the resolution of ambiguous velocity is resolved by the coarse velocity. The strategy provides high enough precision for the radial velocity and decreases the burden of the radar system.

The remainder of this paper is organized as follows: the signal model is presented in Section 2; the velocity estimation method is proposed in Section 3; simulated and experimental results are illuminated in Section 4; and conclusions are summarized in Section 5.

## 2. SIGNAL MODEL

Figure 1 shows the ISAR geometry. A target moves from A to C as shown in Figure 1(a), which can be divided into three segments. In the first segment, the target circles from A to B as shown in Figure 1(b), which has no effect on ISAR imaging. In the second segment, the target translates from B to C as shown in Figure 1(c), which introduces range misalignment and phase error. Unless an optimal translational motion compensation is obtained, serious blurring and smearing will be in the ISAR image. In the third segment, the target rotates around its center at C as shown in Figure 1(d), which provides the high-resolution in cross-range of target imagery. Hence the target motion can be divided into translation and rotation. Thus, the instantaneous distance from the $k$th scattering center at $(x_k, y_k)$ to radar is given by [24]

$$r_k(t) = R_O(t) + x_k \sin \theta(t) - y_k \cos \theta(t), \tag{1}$$

where $R_O(t)$ denotes instantaneous radial range from radar to the target center, usually corresponding to the translational motion. $\theta(t)$ is the instantaneous rotation angle and $t$ is the slow time.

Assume that the radar transmits a waveform

$$s_T(\tau, t) = u(\tau) \exp(j2\pi f_c t), \tag{2}$$

where $u(\tau)$ is the complex envelope of the transmitted signal, $\tau$ the fast time, and $f_c$ the carrier frequency.

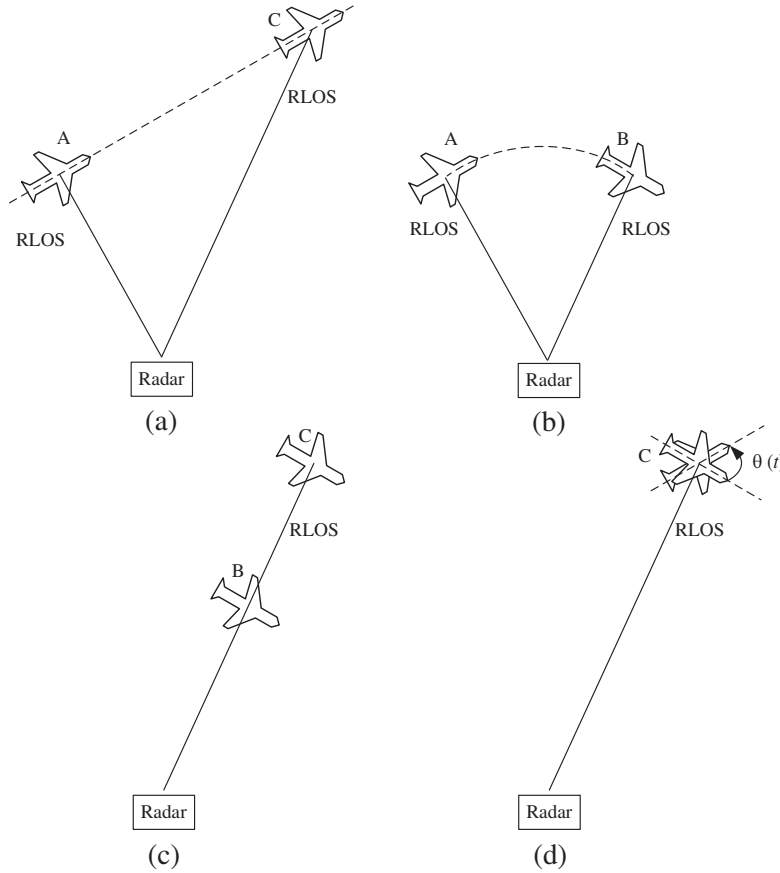Therefore, the received signal from the target after down-conversion to the baseband is given by

$$s_R(\tau, t) = \sum_{k=1}^{K} \delta_k u \left[ \tau - \frac{2r_k(t)}{c} \right] \exp \left[ -j2\pi f_c \frac{2r_k(t)}{c} \right], \tag{3}$$

where $K$ is the total number of the scattering centers, $\delta_k$ the scattering coefficient at $(x_k, y_k)$, and $c$ the light speed.

By applying Fourier transform with respect to $\tau$, we have

$$S_R(f, t) = U(f) \sum_{k=1}^{K} \delta_k \exp \left[ -j2\pi (f + f_c) \frac{2r_k(t)}{c} \right], \tag{4}$$

where $U(f)$ is Fourier transform of $u(\tau)$.

**Figure 1.** ISAR geometry.

After matched-filter correlation processing in pulse compression, the signal is expressed as

$$S(f,t) = |U(f)|^2 \sum_{k=1}^{K} \delta_k \exp\left[-j2\pi(f+f_c)\frac{2r_k(t)}{c}\right].$$  (5)

By substituting Eq. (1) into Eq. (5) and neglecting the constants, we have

$$S(f,t) = \sum_{k=1}^{K} \delta_k \exp\left[-j4\pi(f+f_c)\frac{x_k\sin\theta(t)-y_k\cos\theta(t)}{c}\right]\exp\left[-j2\pi f\frac{2R_O(t)}{c}\right]\exp\left[-j2\pi f_c\frac{2R_O(t)}{c}\right].$$  (6)

In Eq. (6), the term $\exp[-j2\pi f\frac{2R_O(t)}{c}]$ causing misalignment of HRRP in the range-compressed domain needs range alignment. And the term $\exp[-j2\pi f_c\frac{2R_O(t)}{c}]$ standing for the phase error requires phase adjustment. They are just two typical steps of translational motion compensation.

## 3. VELOCITY ESTIMATION

Equation (6) shows that both the range migration and phase error correspond to the translational motion $R_O(t)$. When an optimal translational motion compensation is achieved, the translational motion information $R_O(t)$ can be obtained. Once the instantaneous radial range $R_O(t)$ is known, the radial velocity is just the range differential.

However, it is not the situation for stretch processing, where the signal model can be expressed in

frequency domain as [23]:

$$S_{\text{str}}(f, t) = \sum_{k=1}^{K} \delta_k T_p \text{sinc}\left[\gamma T_p\left(\frac{f}{\gamma} + 2\frac{R_\Delta}{c}\right)\right] \exp\left[-j4\pi f_c \frac{x_k \sin\theta(t) - y_k \cos\theta(t)}{c}\right]$$

$$\exp\left[-j2\pi f_c \frac{2R_O(t)}{c}\right] \exp\left[j2\pi f_c \frac{2R_{\text{ref}}(t)}{c}\right], \tag{7}$$

where $T_p$ is the pulse duration, $\gamma$ the chirp rate, $R_\Delta = r_k(t) - R_{\text{ref}}(t)$, and $R_{\text{ref}}(t)$ the reference distance. Hence the reference distance introduces additional errors. Since the reference distance changes with the position of the target, the range migration and phase error do not correspond to the translational motion $R_O(t)$ any more. In other words, the instantaneous radial range $R_O(t)$ cannot be obtained by the translational motion compensation.

It should be noted that compensations of the range misalignment and phase error require different precisions. To remove the profile migration through range cells, the precision of the range shift should be in the order of a fraction of a range cell, such as a quarter of one range cell, which is typically tens of centimeters. However, the phase error corresponds to the radar operating wavelength, which is typically only a few centimeters. Limited by the range resolution, the motion estimate from range alignment is insufficient to perform an optimal phase adjustment. Moreover, due to the shortness of the wavelength, the phase errors are largely wrapped, resulting in the uncertainty between the phase error and $R_O(t)$ [24]. Therefore, range alignment is applied to get the radial range shift and then the velocity, which is coarse but unambiguous. Then, phase adjustment is performed to obtain the range shift and then the velocity, which is fine but ambiguous. Finally, ambiguity resolution is carried out.

Rewrite Eq. (6) in a discrete form as

$$S(n, m) = \sum_{k=1}^{K} \delta_k \exp\left[-j4\pi\left(n\Delta f + f_c\right)\frac{x_k \sin\theta(m) - y_k \cos\theta(m)}{c}\right]$$

$$\exp\left[-j2\pi n\Delta f\frac{2R_O(m)}{c}\right] \exp\left[-j2\pi f_c \frac{2R_O(m)}{c}\right], \tag{8}$$

where $n$ is the range cell number, $m$ the pulse number, $\Delta f$ the resolution of frequency, and $R_O(m)$ and $\theta(m)$ are the radial range and rotation angle corresponding to the $m$th pulse, respectively.

Range alignment is to compensate the range shifts of profiles. There have been many methods to perform range alignment [25–27]. Denote $s(m)$ and $s(m+1)$ as the adjacent profiles corresponding to the $m$th and $(m+1)$th pulses, respectively. After range alignment, the range shift of the two profiles is obtained, assuming to be $\Delta n(m)$ range cell, which means that

$$R_O(m+1) - R_O(m) = \Delta n(m) \cdot \rho_r, \tag{9}$$

where $\rho_r$ is the resolution of range cell. Then the coarse but unambiguous radial velocity corresponding to the $m$th pulse is given by

$$v_{\text{RA}}(m) = \Delta n(m) \cdot \rho_r \cdot \text{PRF}, \tag{10}$$

where PRF is the pulse repetition frequency.

Phase adjustment is to remove the error phase after range alignment is done well. There have been a lot of schemes to carry out phase adjustment [28–32]. After phase adjustment, the phase error of two aligned adjacent echoes is achieved, assumed to be $\Delta\varphi(m)$ rad, which means that

$$R_O(m+1) - R_O(m) = [\Delta\varphi(m) + 2\pi X_m] \cdot \frac{\lambda}{4\pi}, \tag{11}$$

where $\lambda$ is the radar operating wavelength, and $X_m$ is an integer to ensure $-\pi \leq \Delta\varphi(m) \leq \pi$. Then the precise but ambiguous radial velocity corresponding to the $m$th pulse is given by

$$v_{\text{PA}}(m) = \Delta\varphi(m) \cdot \frac{\lambda}{4\pi} \cdot \text{PRF}. \tag{12}$$

As the error of $\Delta\varphi(m)$ obtained by phase adjustment can be less than $0.25\pi$ rad, corresponding to a radial range deviation of $\lambda/16$ [33], the precision of $v_{\text{PA}}(m)$ is high.

Denote

$$v_{\text{un}} = \frac{\lambda}{2} \cdot \text{PRF}. \tag{13}$$

Then the precise and unambiguous velocity estimation will be

$$v(m) = v_{\text{PA}}(m) + X_m \cdot v_{\text{un}}. \tag{14}$$

Hence, the ambiguity resolution is to determine $X_m$. In order to resolve the ambiguity, the error range of velocity used for ambiguity resolution should be within

$$\left[ -\frac{v_{\text{un}}}{2}, \quad \frac{v_{\text{un}}}{2} \right]. \tag{15}$$

As $v_{\text{RA}}(m)$ is the coarse velocity, $v(m)$ can also be

$$v(m) = v_{\text{RA}}(m) + \varepsilon_1(m), \tag{16}$$

where $\varepsilon_1(m)$ is the error of $v_{\text{RA}}(m)$. As the precision of range shift $\Delta n(m)$ is in the order of a fraction of a range cell, such as a quarter of one range cell, the error range of $v_{\text{RA}}(m)$ is

$$\varepsilon_1(m) \in \left[ -\frac{\rho_r}{4} \cdot \text{PRF}, \quad \frac{\rho_r}{4} \cdot \text{PRF} \right]. \tag{17}$$

Since the resolution of range cell is limited, the precision of $v_{\text{RA}}(m)$ is low. For a typical X-band radar, the operating wavelength is $0.03\,\text{m}$, and the bandwidth is $1\,\text{GHz}$, providing a range resolution of $0.15\,\text{m}$. Then according to Eqs. (15) and (17), $v_{\text{RA}}(m)$ cannot be used for ambiguity resolution.

As the translational motion of ISAR target is regular and during a short dwell time, the translational motion can be approximated effectively by means of a second or third order polynomial. Therefore the precision of $v_{\text{RA}}(m)$ can be improved by polynomial curve fitting. Assuming the velocity after polynomial curve fitting is $v_{\text{RA\_fit}}(m)$, $v(m)$ can be written as

$$v(m) = v_{\text{RA\_fit}}(m) + \varepsilon_2(m), \tag{18}$$

where $\varepsilon_2(m)$ is the error of $v_{\text{RA\_fit}}(m)$, which satisfies the requirement of ambiguity resolution now.

According to Eqs. (14) and (18), $X_m$ is determine by

$$X_m = \left\lceil \frac{v_{\text{RA\_fit}}(m) - v_{\text{PA}}(m)}{v_{\text{un}}} \right\rceil, \tag{19}$$

where $\lceil \cdot \rceil$ denotes for rounding operation.

Hence, the high precise and unambiguous velocity estimation is

$$v(m) = v_{\text{PA}}(m) + \left\lceil \frac{v_{\text{RA\_fit}}(m) - v_{\text{PA}}(m)}{v_{\text{un}}} \right\rceil \cdot v_{\text{un}}. \tag{20}$$

We can obviously see that the precision of the final velocity estimation depends on the precision of $v_{\text{PA}}(m)$. Thus, the proposed method has the high precision with the radial range error less than $\lambda/16$, which is better than other methods [2, 15].

For clarity, we present a flowchart of the proposed algorithm in Figure 2.

## 4. SIMULATIONS AND EXPERIMENTS

This section intends to validate the algorithm performance using simulated data of a target with four scattering centers as well as real radar measurement data of an aircraft.

Let's begin by referring to Figure 3, which is a gray-scale plot of the simulated two-dimensional target. For this simulation, each of the point scatterers has equal reflectivity and the target has a uniformly accelerated translation and uniform rotation. The simulation parameters including the radar characteristics and the target motion quantities are shown in Table 1.

Figure 4 shows the sequences of HRRP. We can easily note that the traces of the time history of the scatterers are almost linear, which indicate the translational motion information.

The range shifts, obtained by range alignment, are provided in Figure 5. And the corresponding coarse velocities are shown as the dashed line in Figure 6. Though the curve of range shifts seems
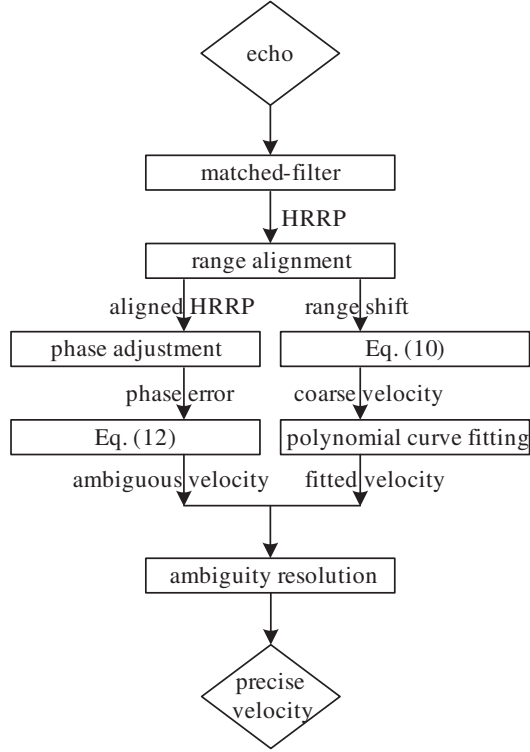
**Figure 2.** Flowchart of the proposed algorithm.

**Table 1.** Simulation parameters.

| Carrier frequency | 10 GHz |
|---|---|
| Bandwidth | 1 GHz |
| Pulse repetition frequency | 166 Hz |
| Sampling rate | 1.2 GHz |
| Echo numbers | 100 |
| Range cell numbers | 2048 |
| Initial range | 15 km |
| Initial velocity | 200 m/s |
| Acceleration | 20 m/s$^2$ |
| Rotation velocity | 1.08 deg/s |

smooth, the velocity curve is rough, as a result of the limited range resolution and the performance of range alignment. According to the radar parameters, the error of coarse velocity for ambiguity resolution should be no more than 1.245 m/s. Hence such coarse velocities cannot be used for ambiguity resolution. The solid line plotted in Figure 6 is the velocity curve after polynomial curve fitting, which is smooth.

The phase errors, achieved by phase adjustment, are shown in Figure 7. We can see that the phase errors are wrapped. Hence, the derived velocities are ambiguous as shown in Figure 8.

After ambiguity resolution using the fitted velocities, the precise velocities are presented as shown as the solid line in Figure 9(a). The dash-dot line displayed in Figure 9(b) is the simulated theoretical velocities. The two lines almost coincide. In order to compare them, the velocity errors are shown as the solid line in Figure 10, which are on the order of $10^{-4}$ m/s. The root mean square error (RMSE)
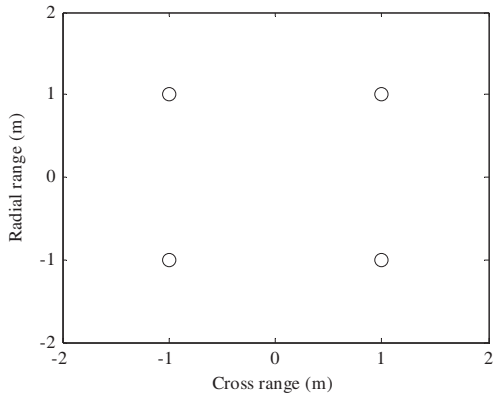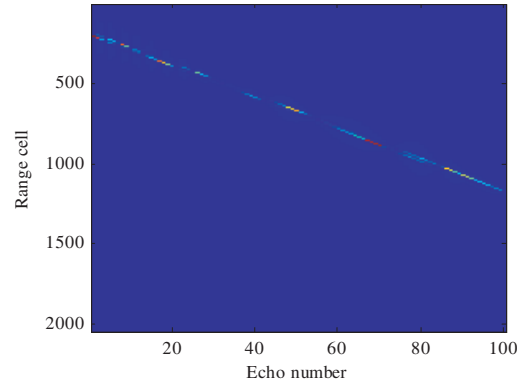
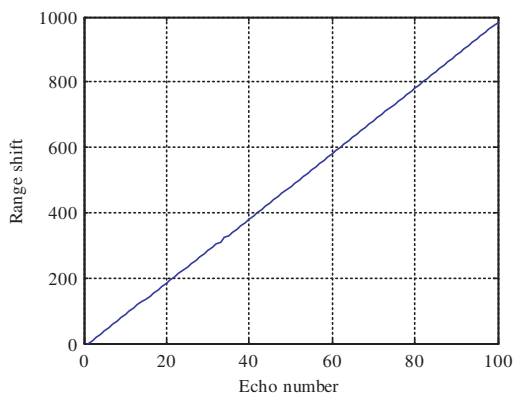**Figure 3.** Simulated target.



**Figure 4.** Sequences of HRRP.



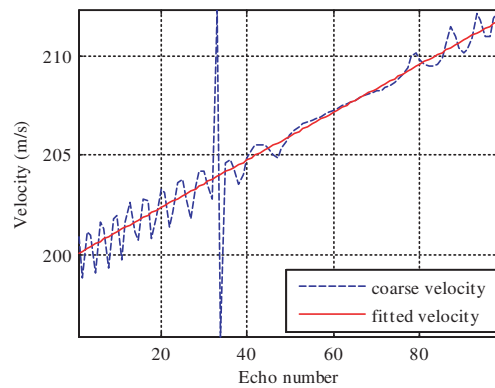**Figure 5.** Range shifts.



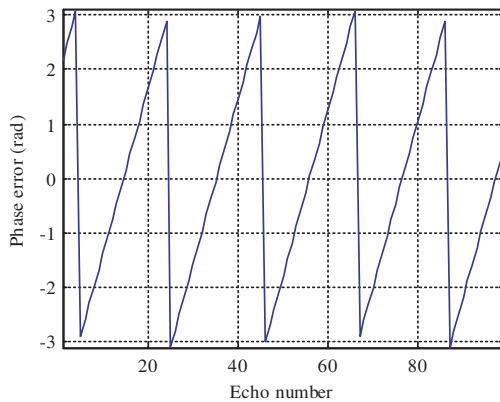**Figure 6.** Coarse velocities and fitted velocities.
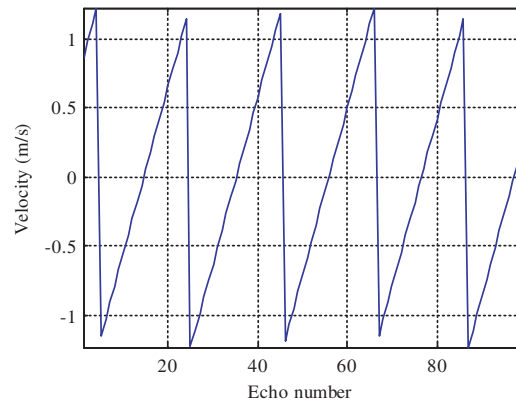


**Figure 7.** Phase errors.



**Figure 8.** Ambiguous velocities.

is calculated to be $1.696 \times 10^{-4}$ m/s. The performance of the proposed method is further compared to that of a robust and computationally efficient technique named Translational Motion Estimation and Compensation (TMEC) [15]. The dash-dot line shown in Figure 10 is the velocity errors of TMEC, which are on the order of $10^{-3}$ m/s. The RMSE is calculated to be $6.907 \times 10^{-3}$ m/s. It is obvious that the velocity errors of the proposed method are smaller than those of TMEC. Hence, the effectiveness of the proposed algorithm is validated.

Further, the performance of the proposed method under different signal-to-noise ratio (SNR) conditions is considered. For simplicity, we do not consider noise in the above simulation. However, noise is present in real life situations. Hence we add noise into the signal to generate SNR varying from
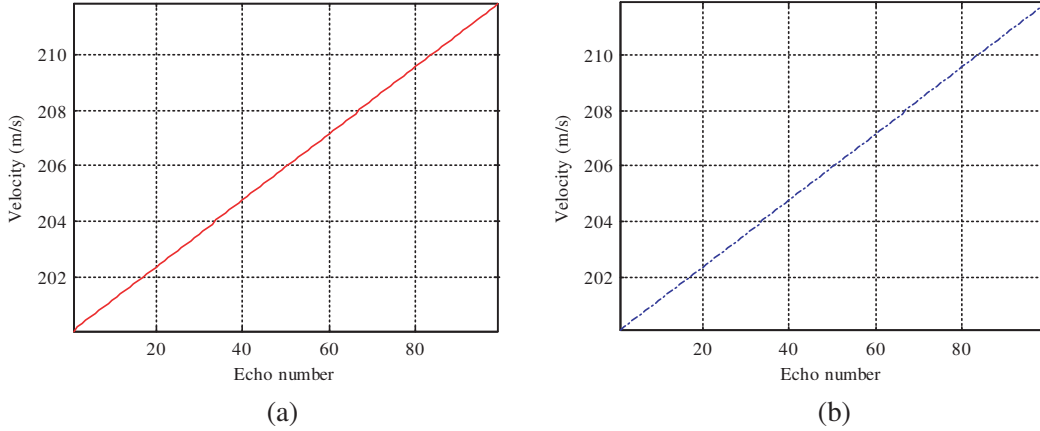
**Figure 9.** Velocity comparison. (a) Estimated velocity. (b) Theoretical velocity.
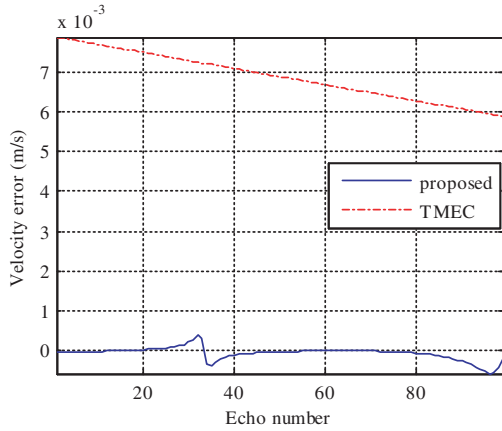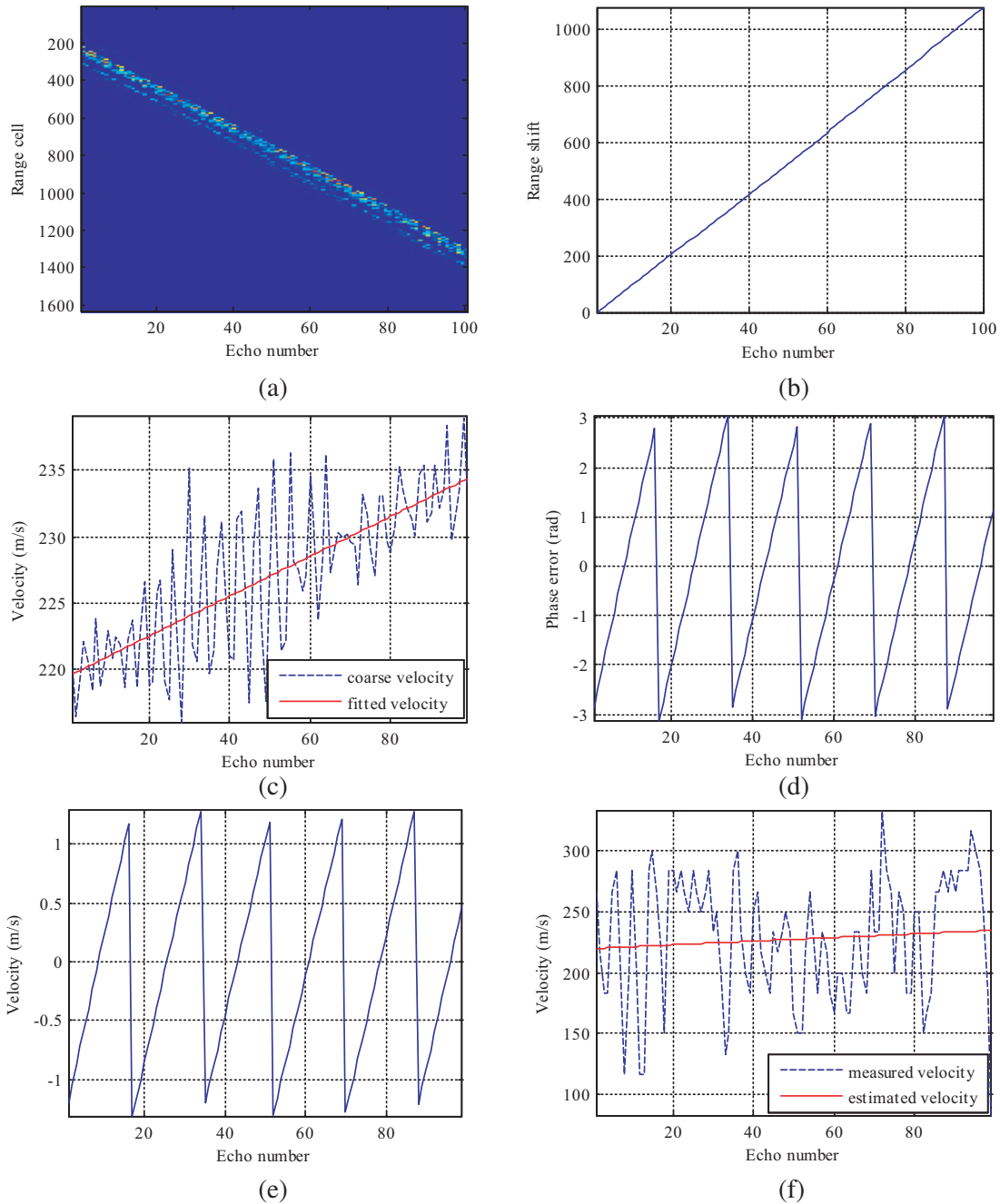


**Figure 10.** Velocity errors.
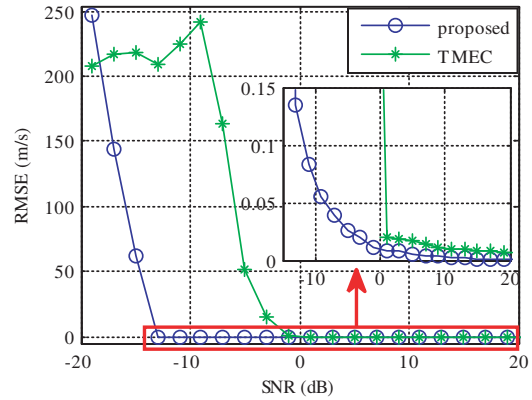
**Figure 11.** RMSEs under different SNRs.

$-20$ to $20$ dB with a step of $2$ dB in the following simulation. The noise is additive Gaussian white noise with a mean of zero. The simulation is carried out and the RMSE of the velocity estimation is calculated at every SNR condition. Figure 11 shows the RMSEs corresponding to different SNRs, which presents that the proposed method provides very small RMSE when SNR is above $-13$ dB, demonstrating that the proposed method is effective, even in a low SNR case. It can also be seen that the RMSEs of the proposed method are lower than those of TMEC, which further verifies the effectiveness of the proposed method.

Real radar data of a non-cooperative aircraft are utilized to further validate the performance of the proposed method. The target is a Boeing 737 aircraft, which has the length/width/height of $33.6$ m/$34.3$ m/$12.5$ m, respectively. The aircraft has just taken off and is accelerating. The distance between the aircraft and the radar is about $38$ km. The aircraft is measured by the X-band radar under field conditions. The parameters of the radar are as follows: the center frequency is $10$ GHz; the bandwidth is $1$ GHz; and the PRF is $166$ Hz. Thus the range resolution is $0.15$ m, and the maximum error of $v_{RA}(m)$ is $6.225$ m/s, while the operating wavelength is $0.03$ m and the error of coarse velocity for ambiguity resolution should be no more than $1.245$ m/s.

Results of real radar data, shown in Figure 12, are very similar to the simulation results. Figure 12(a) shows the sequences of HRRP and (b) is the range shifts obtained by range alignment. The corresponding coarse velocities are shown as the dashed line in Figure 12(c) while the velocities after polynomial curve fitting as the solid line. The phase errors achieved by phase adjustment are shown in Figure 12(d) and the derived velocities are in (e). The final precise velocities are presented as the solid line in Figure 12(f), where the dashed line is the velocities measured by the narrowband mode. From this comparison, the effectiveness of the proposed algorithm is verified.

**Figure 12.** Results of real radar data. (a) Sequences of HRRP. (b) Range shifts. (c) Coarse velocities and fitted velocities. (d) Phase errors. (e) Ambiguous velocities. (f) Velocity comparison.

## 5. CONCLUSION

A convenient technique for estimating radial velocity has been proposed in this paper. The method estimates the precise velocity directly from the wideband echoes by range alignment and phase adjustment, which are the two steps of translational motion compensation in ISAR imaging. Thus it has the advantage of high precision and decreases the burden of the radar system. Results based on simulated and measured data have validated the performance of the proposed algorithm.

## ACKNOWLEDGMENT

## REFERENCES

1. Abatzoglou, T. J. and G. O. Gheen, "Maximum likelihood motion compensation of a wideband linear FM radar waveform," *The Thirtieth Asilomar Conference on Signals, Systems and Computers*, Vol. 1, 481–485, CA, USA, Nov. 3–6, 1996.

2. Liu, Y., S. Zhang, D. Zhu, and X. Li, "A novel speed compensation method for ISAR imaging with low SNR," *Sensors*, Vol. 2015, No. 15, 18402–18415, Jul. 2015.

3. Camp, W. W., J. T. Mayhan, and R. M. O'Donnell, "Wideband radar for ballistic missile defense and Range-Doppler imaging for satellites," *Lincoln Laboratory Journal*, Vol. 12, No. 2, 267–280, Feb. 2000.

4. Delaney, W. P. and W. W. Ward, "Radar development at Lincoln Laboratory: An overview of the first fifty years," *Lincoln Laboratory Journal*, Vol. 12, No. 2, 147–166, Feb. 2000.

5. Steudel, F., "An improved process for Phase-Derived-Range measurements," World Intellectual Property Organization Patent, WO 2005 017 553A1, Feb. 24, 2005.

6. Steudel, F., "Process for Phase-Derived-Range measurements," U.S. Patent 2005 030 222A1, Feb. 10, 2005.

7. Cao, Y., X. Qu, and P. Huang, "Accurate-velocity-measurement method for wideband radar based on keystone transform," *Systems Engineering and Electronics*, Vol. 31, No. 1, 1–4, Jan. 2009.

8. Liu, H. and J. Lu, "Target motion compensation algorithm based on keystone transform for wideband pulse Doppler radar," *Transactions of Beijing Institute of Technology*, Vol. 32, No. 6, 625–630, Jun. 2012.

9. Li, Y., M. Xing, J. Su, Y. Quan, and Z. Bao, "A New algorithm of ISAR imaging for maneuvering targets with low SNR," *IEEE Transactions on Aerospace and Electronic Systems*, Vol. 49, No. 1, 543–557, Jan. 2013.

10. Liu, Y., H. Meng, G. Li, and X. Wang, "Velocity estimation and range shift compensation for high range resolution profiling in stepped-frequency radar," *IEEE Geoscience and Remote Sensing Letters*, Vol. 7, No. 4, 791–795, Oct. 2010.

11. Berizzi, F., M. Martorella, A. Cacciamano, et al., "A contrast-based algorithm for synthetic range profile motion compensation," *IEEE Transactions on Geoscience and Remote Sensing*, Vol. 46, No. 10, 3053–3062, Oct. 2008.

12. Liu, Y., D. Zhu, X. Li, and Z. Zhuang, "Micromotion characteristic acquisition based on wideband radar phase," *IEEE Transactions on Geoscience and Remote Sensing*, Vol. 52, No. 6, 3650–3657, Jun. 2014.

13. Zhu, D., Y. Liu, K. Huo, and X. Li, "A novel high-precision phase-derived-range method for direct sampling LFM radar," *IEEE Transactions on Geoscience and Remote Sensing*, Vol. 54, No. 2, 1131–1141, Feb. 2016.

14. Song, P., H. Meng, T. Huang, and Y. Liu, "A novel target motion compensation method for randomized stepped frequency ISAR," *2013 Asilomar Conference on Signals, Systems and Computers*, 917–921, Pacific Grove, CA, Nov. 3–6, 2013.

15. Mohapatra, B. B., S. Rajagopal, and V. A. Abid Hussain, "Translational motion estimation and compensation in inverse synthetic aperture radar," *2014 IEEE International Conference on Electronics, Computing and Communication Technologies*, 1–5, Bangalore, Jan. 6–7, 2014.

16. Kathree, U., W. Nel, V. J. van Rensburg, and A. K. Mishra, "Investigation of hopped frequency waveforms for range and velocity measurements of radar targets," *2015 IEEE Radar Conference*, 475–480, Johannesburg, Oct. 27–30, 2015.

17. Bucciarelli, M., D. Pastina, B. Errasti-Alcala, and P. Braca, "Translational velocity estimation by means of bistatic ISAR techniques," *2015 IEEE International Geoscience and Remote Sensing Symposium*, 1921–1924, Milan, Jul. 26–31, 2015.

18. Brisken, S. and J. G. Worms, "ISAR motion parameter estimation via multilateration," *2011 Microwaves, Radar and Remote Sensing Symposium*, 190–194, Kiev, Ukraine, Aug. 25–27, 2011.

19. Corretja, V., E. Grivel, Y. Berthoumieu, J. M. Quellec, T. Sfez, and S. Kemkemian, "Target radial velocity estimation robust against additive disturbances for ISAR application," *2011 IEEE CIE International Conference on Radar*, 670–673, Chengdu, China, Oct. 24–27, 2011.

20. Berger, T. and S. E. Hamran, "An efficient scaled maximum likelihood algorithm for translational motion estimation in ISAR imaging," *2010 IEEE Radar Conference*, 75–80, Washington, DC, May 10–14, 2010.

21. Aprile, A., D. Meledandri, T. M. Pellizzeri, and A. Mauri, "A new approach for estimation and compensation of target translational motion in ISAR imaging," *2008 IEEE Radar Conference*, 1–6, Rome, May 26–30, 2008.

22. Lin, Q., B. Yuan, Y. Zhang, and Z. Chen, "Design and implementation of IF signal highspeed acquisition and real-time storage system for wideband radar," *2011 International Conference on Mechatronic Science, Electric Engineering and Computer*, 2022–2026, Jilin, China, Aug. 19–22, 2011.

23. Lin, Q., Z. Chen, Y. Zhang, and J. Lin, "Coherent phase compensation method based on direct IF sampling in wideband radar," *Progress In Electromagnetics Research*, Vol. 136, 753–764, 2013.

24. Zhang, L., J. Sheng, J. Duan, et al., "Translational motion compensation for ISAR imaging under low SNR by minimum entropy," *EURASIP Journal on Advances in Signal Processing 2013*, Vol. 2013, No. 33, 1–19, 2013.

25. Chen, C. C. and H. C. Andrews, "Target-motion-induced radar imaging," *IEEE Transactions on Aerospace and Electronic Systems*, Vol. 16, No. 1, 2–14, Jan. 1980.

26. Wang, J. and D. Kasilingam, "Global range alignment for ISAR," *IEEE Transactions on Aerospace and Electronic Systems*, Vol. 39, No. 1, 351–357, Jan. 2003.

27. Zhu, D., L. Wang, Y. Yu, Q. Tao, and Z. Zhu, "Robust ISAR range alignment via minimizing the entropy of the average range profile," *IEEE Geoscience and Remote Sensing Letters*, Vol. 6, No. 2, 204–208, Apr. 2009.

28. Itoh, T. M. and G. W. Donohoe, "Motion compensation for ISAR via centroid tracking," *IEEE Transactions on Aerospace and Electronic Systems*, Vol. 32, No. 7, 1191–1197, Jul. 1996.

29. Ye, W., T. S. Yeo, and Z. Bao, "Weighted least-squares estimation of phase errors for SAR/ISAR autofocus," *IEEE Transactions on Geosciences and Remote Sensing*, Vol. 37, No. 9, 2487–2494, Sep. 1999.

30. Eichel, P. H. and C. V. Jakowatz, "Phase-gradient algorithm as an optimal estimator of the phase derivative," *Optics Letters*, Vol. 14, No. 20, 1101–1103, 1989.

31. Li, X., G. Liu, and J. Ni, "Autofocusing of ISAR imaging based on entropy minimization," *IEEE Transactions on Aerospace and Electronic Systems*, Vol. 35, No. 4, 1240–1251, Apr. 1999.

32. Martorella, M., F. Berizzi, and B. Haywood, "Contrast maximization based technique for 2-D ISAR autofocusing," *IEE Proceedings on Radar, Sonar and Navigation*, Vol. 52, No. 4, 253–262, Apr. 2005.

33. Xu, R., Z. Cao, and Y. Liu, "A new method of motion compensation for ISAR," *1990 IEEE International Radar Conference*, 234–237, Arlington, VA, May 7–10, 1990.